**DOI:** 10.21122/2220-9506-2026-17-2-108-116

# Experimental Evaluation of Damping Suspension Performance for Unmanned Aerial Vehicle Camera Equipment Using Combined Optical Flow and Inertial Sensor Analysis

**A.A. Lamaka, L.V. Katkovsky, P.V. Ivuts, A.V. Damaratski, N.G. Shcherbakou**

*A.N. Sevchenko Institute of Applied Physical Problems of Belarusian State University, Kurchatov str., 7, Minsk 220045, Belarus*

*Received 08.04.2026*
*Accepted for publication 26.05.2026*

**Abstract**

Ensuring stabilization of imaging equipment onboard unmanned aerial vehicles is a critical factor for the quality of aerial photography and spectrometric measurements, while objective comparative assessment of the effectiveness of various damping suspensions under real flight conditions remains a methodologically challenging task. Aim of this work was an experimental evaluation of the damping suspensions for UAV payloads effectiveness using integrated analysis of IMU data and computer vision. Studies were carried out on a system based on the Matrice 300 RTK unmanned aerial vehicle and a Raspberry Pi data logger. Damping suspensions operating in compression and tension were compared with rigid mounting. Methods used for video stream analysis to determine the amplitude-frequency characteristics of the imaging system orientation angles were described. Data processing methods from the inertial measurement unit to obtain information on the dynamics of orientation angles are indicated. A method for integrated processing of camera and IMU data is disclosed, which allows combining the low-frequency accuracy of optical flow with the broad bandwidth of inertial sensor measurements. The effectiveness of different types of damping suspensions was investigated at drone flight speeds from 1 to 7 m/s. It was found that the best performance was exhibited by a suspension with silicone dampers operating in compression, which reduced the energy of vibration processes by up to 77 % in the range from 0 to 85 Hz.

**Keywords:** angular vibration, spectral analysis, aerial photography, inertial measurements, computer vision

***Адрес для переписки:***
*Ломако А.А.*
*Институт прикладных физических проблем имени А.Н. Севченко Белорусского государственного университета,*
*ул. Курчатова, 7, г. Минск 220045, Беларусь*
*e-mail alekseylomako@gmail.com*

***Address for correspondence:***
*Lamaka A.A.*
*A.N. Sevchenko Institute of Applied Physical Problems of Belarusian State University,*
*Kurchatov str., 7, Minsk 220045, Belarus*
*e-mail alekseylomako@gmail.com*

***Для цитирования:***
A.A. Lamaka, L.V. Katkovsky, P.V. Ivuts, A.V. Damaratski, N.G. Shcherbakou.
Experimental Evaluation of Damping Suspension Performance for Unmanned Aerial Vehicle Camera Equipment Using Combined Optical Flow and Inertial Sensor Analysis.
Приборы и методы измерений.
2026. Т. 17. № 2. С. 108-116.
**DOI:** 10.21122/2220-9506-2026-17-2-108-116

***For citation:***
Lamaka AA, Katkovsky LV, Ivuts PV, Damaratski AV, Shcherbakou NG.
Experimental Evaluation of Damping Suspension Performance for Unmanned Aerial Vehicle Camera Equipment Using Combined Optical Flow and Inertial Sensor Analysis.
*Devices and Methods of Measurements.*
2026;17(2):108-116.
**DOI:** 10.21122/2220-9506-2026-17-2-108-116

**DOI:** 10.21122/2220-9506-2026-17-2-108-116

# Экспериментальное исследование работы демпферных подвесов для съёмочной аппаратуры беспилотных летательных аппаратов на основе комплексного анализа оптического потока и сигналов инерциальных датчиков

**А.А. Ломако, Л.В. Катковский, П.В. Ивуть, А.В. Домарацкий, Н.Г. Щербаков**

*Институт прикладных физических проблем имени А.Н. Севченко*
*Белорусского государственного университета,*
*ул. Курчатова, 7, г. Минск 220045, Беларусь*

*Поступила 08.04.2026*
*Принята к печати 26.05.2026*

Обеспечение стабилизации съёмочной аппаратуры на борту беспилотных летательных аппаратов является критическим фактором качества аэрофотосъёмки и спектрометрических измерений, при этом объективная сравнительная оценка эффективности различных демпферных подвесов в реальных условиях полёта остаётся методически сложной задачей. Целью работы являлась экспериментальная оценка эффективности демпферных подвесов для полезной нагрузки беспилотных летательных аппаратов с использованием комплексного анализа данных инерциального измерительного модуля и компьютерного зрения. Исследования выполнены на комплексе с беспилотным летательным аппаратом *Matrice* 300 *RTK* и регистратором данных на *Raspberry Pi*. Демпферные подвесы, работающие на сжатие и растяжение, сравнивались с жёстким креплением. Описываются использованные методы анализа видеопотока для определения амплитудно-частотных характеристик углов ориентации съёмочной системы. Указываются методы обработки данных инерциального измерительного модуля для получения информации о динамике углов ориентации. Раскрывается методика комплексной обработки данных камеры и инерциального блока, позволяющая объединить низкочастотную точность оптического потока и широкополосность измерений инерциальных датчиков. Проводились исследования эффективности работы типов демпферных подвесов на скоростях полёта дрона от 1 до 7 м/с. Установлено, что лучшей эффективностью обладает подвес с силиконовыми демпферами, работающими на сжатие, который позволяет уменьшать энергию вибрационных процессов на величину до 77 % в диапазоне от 0 до 85 Гц.

**Ключевые слова:** угловая вибрация, спектральный анализ, аэрофотосъёмка, инерционные измерения, компьютерное зрение

***Адрес для переписки:***
*Ломако А.А.*
*Институт прикладных физических проблем имени А.Н. Севченко*
*Белорусского государственного университета,*
*ул. Курчатова, 7, г. Минск 220045, Беларусь*
*e-mail alekseylomako@gmail.com*

***Address for correspondence:***
*Lamaka A.A.*
*A.N. Sevchenko Institute of Applied Physical Problems of Belarusian State University,*
*Kurchatov str., 7, Minsk 220045, Belarus*
*e-mail alekseylomako@gmail.com*

***Для цитирования:***
A.A. Lamaka, L.V. Katkovsky, P.V. Ivuts, A.V. Damaratski, N.G. Shcherbakou.
Experimental Evaluation of Damping Suspension Performance for Unmanned Aerial Vehicle Camera Equipment Using Combined Optical Flow and Inertial Sensor Analysis.
Приборы и методы измерений.
2026. Т. 17. № 2. С. 108-116.
**DOI:** 10.21122/2220-9506-2026-17-2-108-116

***For citation:***
Lamaka AA, Katkovsky LV, Ivuts PV, Damaratski AV, Shcherbakou NG.
Experimental Evaluation of Damping Suspension Performance for Unmanned Aerial Vehicle Camera Equipment Using Combined Optical Flow and Inertial Sensor Analysis.
*Devices and Methods of Measurements.*
2026;17(2):108-116.
**DOI:** 10.21122/2220-9506-2026-17-2-108-116

## Introduction

In the last decade, there has been a notable increase in the use of unmanned aerial vehicles (UAVs) in science and industry [1, 2]. Lower risks to personnel and reduced operational costs compared to traditional methods allow unmanned systems to be effectively used in smart city concepts and emergency situations [2]. One catalyst for this development is the use of artificial intelligence models for controlling both the aircraft itself and for solving applied tasks [1, 2]. The integration of deep learning technologies with mobile platforms and data collection sensors is now enabling predictive management in various areas of human activity. However, the simultaneous use of UAVs and scientific equipment in such complex systems requires mitigating the mutual interference between components. Vibrations generated by aircraft operation can cause significant disturbances to sensitive scientific equipment [3, 4]. Vibration compensation systems are generally classified into active and passive types [4]. This work focuses only on passive solutions.

The stability of spectrometric systems installed onboard UAVs is critical for measurement quality [4, 5]. Therefore, selecting the most effective vibration isolation scheme is important for a new hyperspectral automated flight system currently under development. Some studies have calculated damping device parameters based on experimental modal analysis [6]. However, that approach requires additional equipment and expertise. Furthermore, the present study aims to identify the vibration dynamics caused by UAV operation at different flight speeds. Accordingly, it was decided to evaluate the effectiveness of different damper suspension types based on field test results.

The classical approach for experimental assessment of vibration characteristics and intensity involves using an inertial measurement unit (IMU) mounted directly on the carrier UAV or its payload. However, low-cost IMUs, typical for commercial UAVs, exhibit high levels of intrinsic noise and drift [7], which masks the useful vibration signal.

Optical flow from the UAV's onboard camera offers an alternative approach for assessing changes in the orientation of the UAV or its payload over time. Data obtained via computer vision algorithms are drift-free, thus providing better measurement repeatability. However, the frame rate of optical sensors (30–60 Hz) is substantially lower than that of IMUs (hundreds to thousands of hertz), narrowing the spectral range available for analysis. Moreover, according to previous studies, the main natural vibration modes of a UAV with a suspended platform exceed the 15–30 Hz analysis bandwidth available from optical flow alone (in accordance with the Nyquist–Shannon sampling theorem) [6].

When IMU and computer vision methods are used together, the weaknesses of one technology can be compensated for by the strengths of the other, paving the way for a more accurate assessment of different vibration isolation schemes. The aim of this study was to experimentally evaluate the effectiveness of various damper suspension types for UAV payloads using a multi-sensor approach.

## Study instruments

The primary instrument for the research was an unmanned aerial spectrometry complex [5]. It was based on a DJI Matrice 300 RTK UAV[1], with a video-spectral system running on a Raspberry Pi 4 Model B[2] as the payload. The surveillance camera included in the system (a standard Raspberry RGB camera) recorded video at a resolution of 1920×1080 pixels with a frame rate of 30 Hz. The camera's angular resolution was approximately 0.02°, and its field of view was 15°×26°. Due to the specific nature of the task, spectral measurements were not used in this work.

An MPU-6050 sensor[3] was connected to the Raspberry Pi via the I²C interface to serve as the IMU. This chip integrates a 3-axis accelerometer and a 3-axis gyroscope, and includes an embedded digital motion processor. The module was mounted in the same housing as the RGB camera, enabling joint data analysis from the two sensors. The ADC resolution of both the gyroscope and accelerometer was 16 bits. The sampling rate for the experiment was set to 170 Hz. Immediately before the experiments, static IMU measurements (duration > 20 s) were taken to calibrate the sensor bias and determine the scaling factor.

Various suspension designs were used. The base structures were printed on an FDM 3D printer.

[1] UAV DJI Matrice 300 RTK: https://www.dji.com/matrice-300

[2] Raspberry Pi 4: https://www.raspberrypi.com/products/raspberry-pi-4-model-b

[3] IMU MPU-6050: https://product.tdk.com/en/search/sensor/mortion-inertial/imu/info?part_no=MPU-6050

To evaluate vibration loads without vibration compensation, a rigid mount of the payload to the UAV airframe was used (Figure 1*a*). The data obtained under this configuration served as the baseline for comparing the effectiveness of different stabiliser configurations. These configurations can be divided into two types: those operating "in compression" and those operating "in tension".

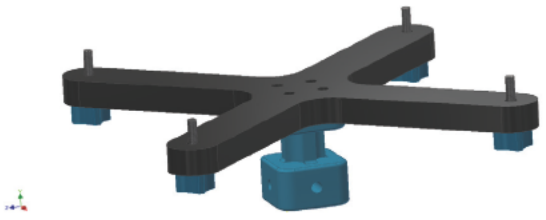

*a*

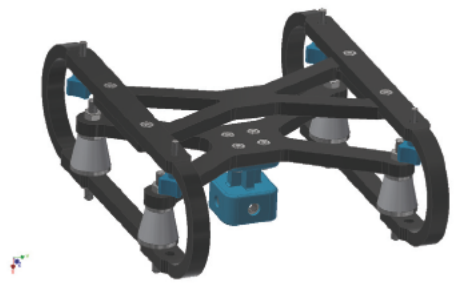

*b*

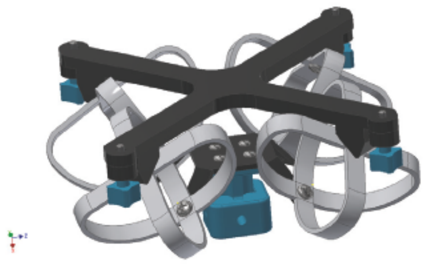

*c*

**Figure 1** – Configurations of rigid equipment mounting (*a*) and two types of damping suspensions: with silicone dampers (*b*) and petal-type (*c*)

In the design that exploits physical principles to resist compression (Figure 1*b*), silicone dampers were used to compensate for vibrations. The size and stiffness of the dampers were selected empirically from commercially available products. In the design based on resistance to tension (Figure 1*c*), specialised petal-type dampers were developed. These were manufactured using filament 3D printing (PETG as the material). The study investigated a petal-type decoupling design in which each of the four dampers had four flexible faces (petals).

## Experimental data processing methods

The video stream processing algorithm consists of several interrelated steps. The raw video is processed using the Lucas–Kanade optical flow algorithm [8], which tracks the displacement of key points between consecutive frames. To detect these points (300 points per frame, with outlier rejection using RANSAC [9]), the Shi–Tomasi corner detector was employed [10]. Based on the obtained point displacements, an affine transformation between frames is computed, from which three key parameters are extracted: linear shifts along the $X$ and $Y$ image axes (corresponding to roll angle $\gamma$ and pitch angle $\theta$) and the rotation angle $\psi$ (yaw). Pixel displacements are converted to angular values using the flight altitude and the camera's spatial resolution:

$$\gamma_V = \operatorname{arctg}\left(dX \cdot R/H\right); \quad \theta_V = \operatorname{arctg}\left(dY \cdot R/H\right), \tag{1}$$

where $\Delta\gamma$ and $\Delta\theta$ are the changes in roll and pitch angles derived from the video stream, $dX$ and $dY$ are pixel shifts along the image axes, $R$ is the spatial resolution per pixel (m/pixel), and $H$ is the flight altitude (m).

To remove the constant component caused by the UAV's horizontal motion, the mean value was subtracted from each time series of angles. This allows focusing on the vibrational component of the oscillations.

To obtain Euler orientation angles from IMU data, sequential processing of accelerometer and gyroscope signals is required. Their combined processing yields accurate angular orientations.

Since the gravity vector is constant, roll and pitch angles can be estimated from accelerometer readings:

$$\gamma_{acc} = \operatorname{arctg}\left(a_y \Big/ \sqrt{a_x^2 + a_z^2}\right); \quad \theta_{acc} = \operatorname{arctg}\left(-a_x \Big/ \sqrt{a_y^2 + a_z^2}\right), \tag{2}$$

where $\gamma_{acc}$ is the roll angle from the accelerometer; $\theta_{acc}$ is the pitch angle from the accelerometer; $a_x$, $a_y$, $a_z$ – are the triaxial accelerometer readings. The *atan*2($y$, $x$) function was used to correctly handle the signs of numerator and denominator, returning an angle in the range ($-\pi$, $\pi$].

The classical approach for joint accelerometer–gyroscope processing is the Kalman filter [12, 13], which compensates for gyroscope drift using accelerometer data. However, in the present work, we deliberately avoided such filtering, as it may distort the amplitude–frequency spectrum of the vibrations under study. Instead, orientation angles from IMU data were obtained by direct integration of the gyroscope signal without any accelerometer correction. Consequently, in the low-frequency range (0–15 Hz), the IMU results contain drift and low-frequency noise, making them less reliable than the drift-free optical flow data.

A distinctive feature of this study is that we do not need to determine the orientation of a non-uniformly moving UAV at every time instant with high precision. Since the ultimate goal is to evaluate the performance of damping suspensions during UAV flight at a given speed, it is sufficient to obtain the amplitude-frequency characteristics (AFC) of the Euler angle oscillations. It is important to note that without any filtering to remove IMU measurement noise, the AFC will contain low-frequency noise components due to sensor drift. Such noise can be compensated by using data from video stream analysis algorithms. Given the video frame rate, this analysis provides the most accurate Euler angle data in the 0–10 Hz range. The intrinsic noise of the IMU sensors will also contribute to the AFC, but this will be broadband background noise common to all experimental measurements, allowing relative comparisons among all results. Moreover, since no filtering is applied during pre-processing, there is no risk of losing informative frequencies characteristic of vibrations. Additionally, the described approach does not require precise temporal synchronization of the IMU and camera readings – with an accumulation time of about 60 s, synchronization to within a few seconds is sufficient, because the spectral characteristics analyzed are time-shift invariant under stationary signal conditions.

To obtain the AFC from both video and IMU data, a time series of the angular deviation magnitude (excluding yaw) is first constructed:

$$M(t) = \sqrt{\gamma^2(t) + \theta^2(t)}. \quad (3)$$

This scalar quantity characterises the intensity of the optical axis deviation from the vertical and is directly related to the image shift magnitude. The yaw oscillation plane is orthogonal to the effective damping suspension direction, so including yaw in the current analysis would only add noise.

Next, a windowed Fourier transform (Welch's method) was applied to the time series calculated with (3). A Hann window of 1024 samples with 50 % overlap was used for IMU data, and 256 samples with 50 % overlap for video-based data. Since IMU and video data have different amplitude scales, they must be brought to a comparable level. For this purpose, a reference frequency range where both methods are considered sufficiently reliable (e. g., 5–10 Hz) was chosen. The median amplitude ratio in this range is computed as:

$$C = \text{median}_{f \in [f_1, f_2]} \left( \frac{S_V(f)}{S_{\text{IMU}}(f)} \right), \quad (4)$$

where $S_V(f)$ is the AFC from video stream data; $S_{\text{IMU}}(f)$ is the AFC from IMU data; $[f_1, f_2]$ is the reference frequency range.

A composite evaluation metric is then formed as:

$$S(f) = \omega(f) \cdot S_V(f) + (1 - \omega(f)) \cdot \overline{C} \cdot S_{\text{IMU}}(f), \quad (5)$$

$\omega(f) = 1 \big/ \left(1 + e^{k(f - f_0)}\right)$ – is a weighting function with transition frequency $f_0$ and steepness coefficient $k$; $\overline{C}$ is the average scaling factor from (4) over all experiments.

The uncertainty of the angular estimate from video is ≈0.02°, while the integrated gyroscope drift reaches ≈0.6° over 60 s, an order of magnitude larger than the amplitude of real low-frequency vibrations. Thus, the form of (5) is justified: video data provide a reliable estimate in the 0–15 Hz band, whereas angles obtained by integrating the IMU gyroscope are less reliable up to 10 Hz due to zero drift. The transition frequency was set to $f_0$ = 7.5 Hz (the midpoint of the video data informative interval), and the steepness coefficient $k$ = 1.2. With these parameters, a smooth transition from full reliance on video to full reliance on IMU occurs in the 5–10 Hz band. Before merging, the video-based data are interpolated onto the IMU frequency grid. It is emphasised that above 15 Hz only IMU data are used; nevertheless, the proposed approach allows consistent scaling and avoids discontinuities at the band boundary.

To compare different suspension types at various UAV flight speeds, integral energy indicators were calculated in selected spectral sub-bands using:

$$E = \sum_{f = f_{\min}}^{f_{\max}} |S(f)|^2, \quad (6)$$

where $f_{\min}$ and $f_{\max}$ are the lower and upper frequency bounds of the analysis band.

The frequency range up to the Nyquist frequency of the IMU data (85 Hz) was divided into conventional sub-bands: low-frequency (Band 1, B1), medium-frequency (Band 2, B2), high-frequency (Band 3, B3), and very-high-frequency (Band 4, B4). The integral energy characteristics were computed according to (6) for each sub-band. The defined sub-bands are listed in Table.

*Table*

**Frequency ranges for integral energy characteristics analysis**

| Диапазоны / ranges | *B*1 | *B*2 | *B*3 | *B*4 |
|---|---|---|---|---|
| $f_{min}$, Гц, Hz | 0 | 15 | 40 | 60 |
| $f_{max}$, Гц, Hz | 15 | 40 | 60 | 85 |

## Experiment and results

To perform the analysis using the method described above, field measurements with a UAV were required. The experiment was organised so that flights were carried out sequentially with different types of damping suspensions installed. For each suspension configuration, flights were conducted at four speeds: 1.5 m/s, 2.5 m/s, 5 m/s, and 7 m/s. The speed range was selected based on typical drone flight speeds at altitudes up to 200 m above ground level. Each measurement lasted between 50 and 70 s. All measurements were taken at a flight altitude of 150 m above the surface. Due to technical issues, flight data for the petal-type suspension at speeds of 1.5 m/s and 2.5 m/s could not be validated.

The first important result is the composite AFC (amplitude-frequency characteristics) calculated using Equation (5) for the rigid mounting of the equipment on the UAV at different flight speeds. This information is essential for determining the baseline conditions for evaluating the effectiveness of the two damping suspension designs. As seen in Figure 2, the characteristics exhibit pronounced peaks in the B3 sub-band. At lower UAV speeds (1.5 and 2.5 m/s), the maxima occur near 45 Hz, while at higher speeds (5 and 7 m/s) the peaks shift to frequencies around 55 Hz. Additionally, peaks appear in the B1 sub-band, whose amplitudes increase with UAV speed. This may be attributed to changes in the UAV rotor operating modes and to the increased influence of wind load on the experimental results at higher flight speeds.

Once the oscillatory behaviour for the rigid mounting case was understood, the next important step was to compare the AFCs obtained with different damping suspensions at specific UAV flight speeds. The most interesting for the purposes of this work are the AFCs at a flight speed of 5 m/s, as this is the optimal speed for the intended payload. Therefore, it is important to qualitatively assess how the AFCs change for different mounting types, which can be seen in the corresponding graphs (Figure 3).

As can be seen in Figure 3, both damping suspension designs attenuate vibrations in the B3 sub-band quite effectively. However, in the B1 sub-band, the silicone damper configuration suppresses oscillation peaks substantially better than the petal-type suspension. Moreover, in the Type B plot, the average amplitude spectrum level decreases across all spectral sub-bands, indicating the overall effectiveness of this damping suspension design. It is worth noting that the scaling factor used to form the composite spectrum via Equation (5) was the same for all three experiments, ensuring the validity of the comparison described above.

To quantitatively compare the effectiveness of the different damping suspension designs, integral energy indicators were calculated using Equation (6) for each UAV flight speed. A graphical representation of the vibration energy dependence on UAV speed in the B1, B2, combined B3+B4 sub-bands, and over the entire 0–85 Hz spectral range is shown in Figure 4.

The analysis of the graphs in Figure 4 should begin with Figure 4*c*, which shows the total energy in the B3 and B4 sub-bands. These two sub-bands were combined because the observed dependencies exhibited similar behaviour. In this spectral region, the silicone damper configuration is the most effective, reducing vibration energy by 52 % (at 7 m/s) to 87 % (at 5 m/s). The petal-type suspension also demonstrates some effectiveness, but the maximum energy reduction achieved was only 26 % (at 7 m/s).

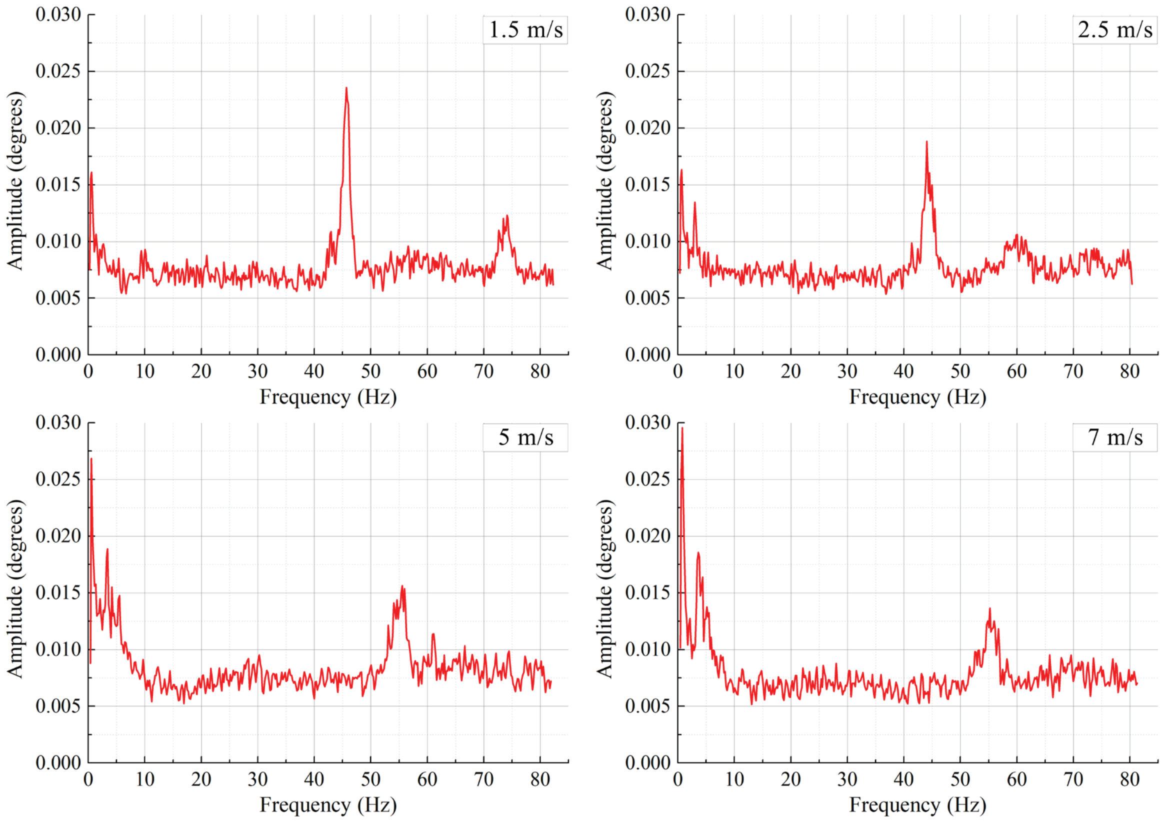


**Figure 2** – Complex amplitude-frequency characteristics of vibrations for the case of rigid mounting of the payload to the unmanned aerial vehicle airframe at different flight speeds

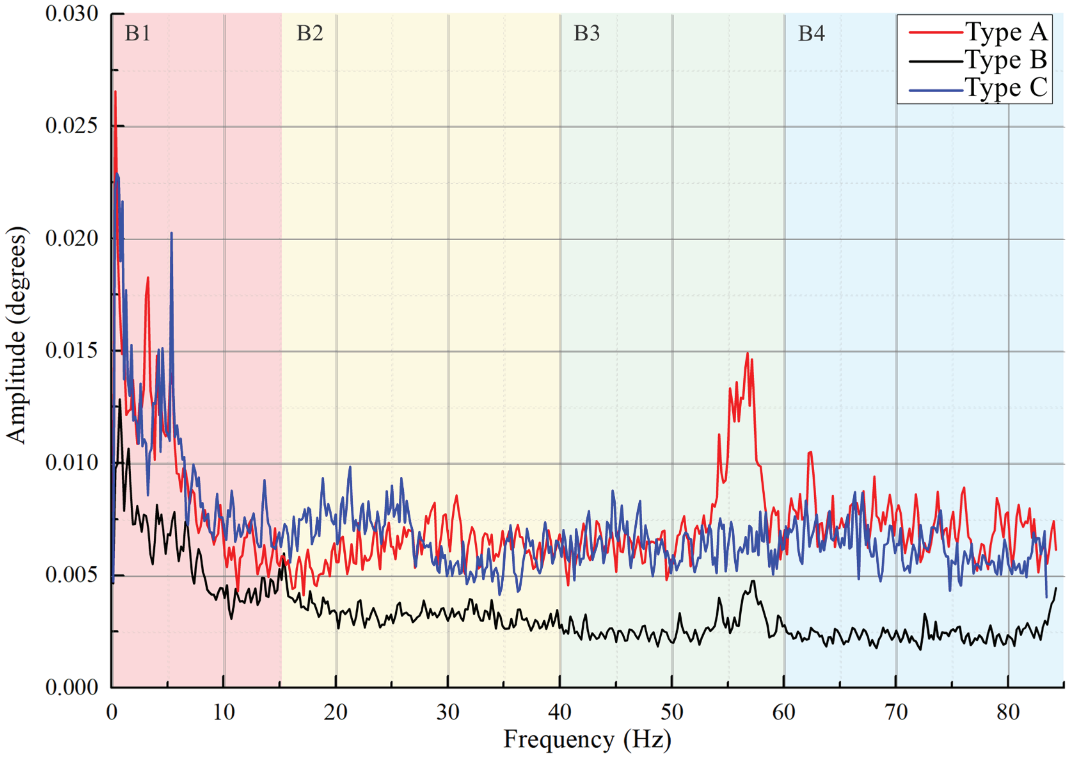


**Figure 3** – Complex amplitude-frequency characteristics of vibrations at the unmanned aerial vehicle flight speed of 5 m/s for three payload mounting types: rigid mounting (*Type A*), suspension with silicone dampers (*Type B*), and petal-type suspension (*Type C*)

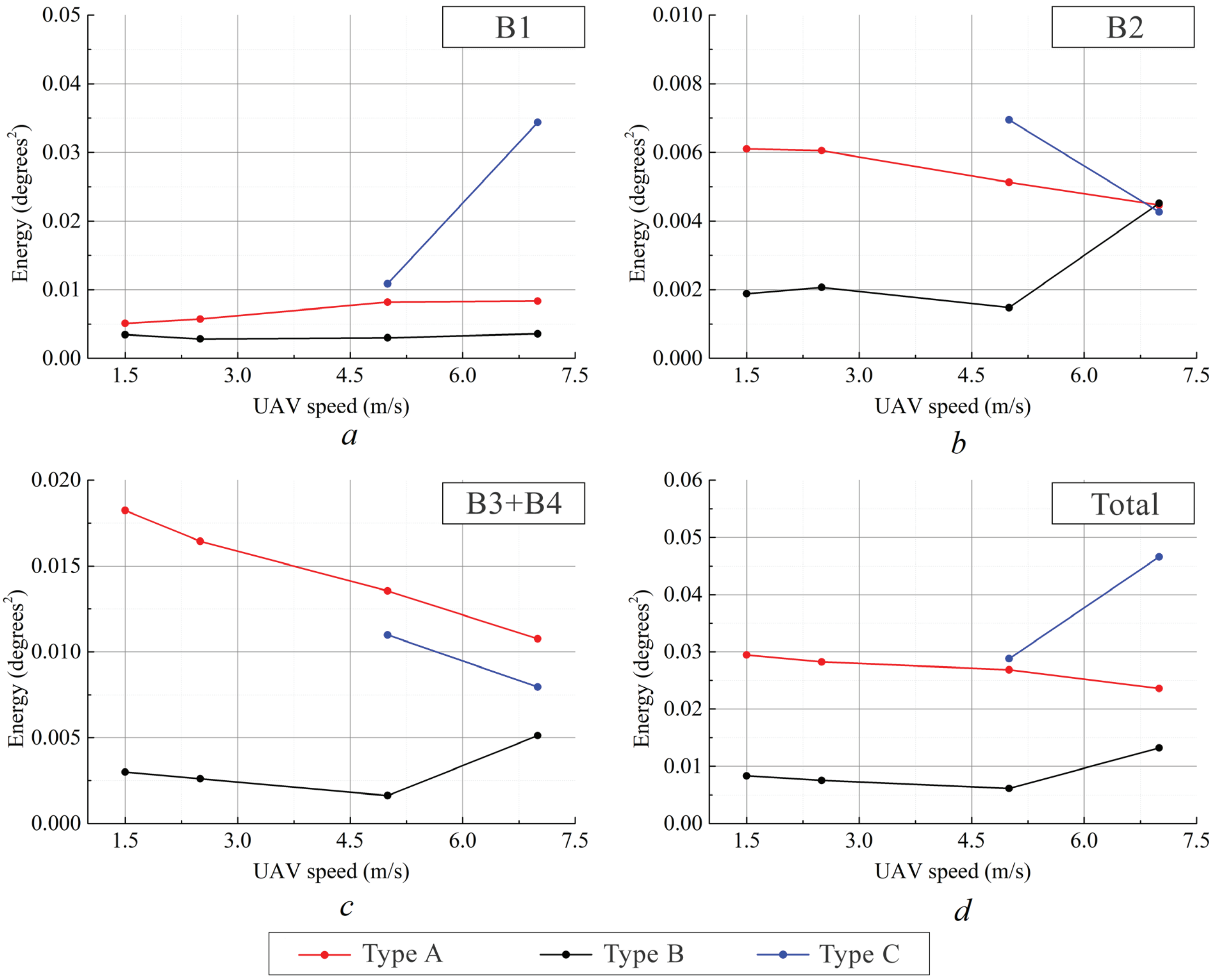


**Figure 4** – Dependencies of integral energy characteristics on the unmanned aerial vehicle flight speed for different types of suspensions in ranges *B*1 (*a*), *B*2 (*b*), *B*3+*B*4 (*c*), and over the entire investigated range (*d*)

Figure 4*b* presents the oscillations in the mid-frequency range. The analysis shows that the vibration level in this sub-band is quite low, and the vibration energy for all mounting configurations is small compared to the other sub-bands. Nevertheless, the silicone damper configuration again exhibits higher efficiency in this sub-band, except at 7 m/s, where all three mounting configurations yield similar values.

As seen in Figure 4*a*, in the B1 sub-band the silicone damper configuration reduces vibration energy by 32 % (at 1.5 m/s) to 63% (at 5 m/s). In contrast, for the petal-type suspension in the same sub-band, the vibration energy increases by 33 % (at 5 m/s) to more than 300 % (at 7 m/s). Such a substantial increase may indicate resonant phenomena occurring with this suspension design.

Analysis of the vibration energy over the entire spectral range (Figure 4*d*) shows that the silicone damper configuration effectively attenuates vibrations induced by UAV operation. The total vibration energy is reduced by 44 % (at 7 m/s) to 77 % (at 5 m/s) when using this configuration. For the petal-type suspension, despite its effective performance in the B3 and B4 sub-bands, the overall vibration energy increases, indicating that this damping suspension design is unsuitable for the present task.

Thus, the proposed evaluation methodology can be used in similar studies to process data from flight tests when standard filtering of IMU signals (e.g., for drift compensation) could distort the spectral composition of the vibrations under investigation. It is important to note that the described integrated use of video and IMU data is not applicable in real-time applications, as it requires processing the entire time series. For such tasks, the classical filtering approach for fusing accelerometer and gyroscope data remains preferable.

## Conclusion

A method for integrated analysis of vibration processes in UAV payloads is proposed, based on video stream data and inertial measurement unit sensors. This method is effective for comparative evaluation of different payload mounting configurations.

When comparing the three mounting configurations (rigid mounting and two damping suspension designs), it was found that at flight speeds up to 7 m/s, the suspension with silicone dampers operating in compression performs best. This suspension reduces vibration energy by up to 77 % in the 0–85 Hz range compared to rigid mounting. The second damping suspension design, although it fulfills its intended function in the high-frequency range (40–85 Hz), is unsuitable for use due to its ineffectiveness in the low-frequency range (up to 15 Hz).

## References

1. Telli K [et al.]. A Comprehensive Review of Recent Research Trends on Unmanned Aerial Vehicles (UAVs). Systems. 2023;(11):400 p.
**DOI:** 10.3390/systems11080400

2. Hildmann H, Kovacs E. Review: Using Unmanned Aerial Vehicles (UAVs) as Mobile Sensing Platforms (MSPs) for Disaster Response, Civil Security and Public Safety. Drones, 2019;(3):59 p.
**DOI:** 10.3390/drones3030059

3. Dogotari M [et al.]. Development of a UAV-Borne LiDAR System for Surveying Applications. Proceedings. 2019;(30):75 p. **DOI:** 10.3390/proceedings2019030075

4. Geronel RS, Botez RM, Bueno DD. On the Effect of Flexibility on the Dynamics of a Suspended Payload Carried by a Quadrotor. Designs. 2022;6(31):2-28.
**DOI:** 10.3390/designs6020031

5. Lamaka AA, Gutarau AV, Shcherbakou NG, Ivuts PV. Photospectral Data Obtaining with the Unmanned Aerial Spectrometry Vehicle. Devices and Methods of Measurements. 2023;14(1):7-17.
**DOI:** 10.21122/2220-9506-2023-14-1-7-17

6. Cocuzza S, Doria A. Modeling and Identification of Vibrations in a UAV for Aerial Manipulation. Advances in Italian Mechanism Science. Mechanisms and Machine Science. 2020;91.
**DOI:** 10.1007/978-3-030-55807-9_21

7. Suvorkin V [et al.]. Assessment of Noise of MEMS IMU Sensors of Different Grades for GNSS/IMU Navigation. Sensors. 2024;24:1953 p.
**DOI:** 10.3390/s24061953

8. Lucas BD, Kanade T. An iterative image registration technique with an application to stereo vision. Proceedings of the 7th International Joint Conference on Artificial Intelligence (IJCAI). 1981;2:674-679 pp.

9. Fischler MA, Bolles RC. Random Sample Consensus: A Paradigm for Model Fitting with Applications to Image Analysis and Automated Cartography. Communications of the ACM. 1981;24(6):381-395.
**DOI:** 10.1145/358669.358692

10. Shi J, Tomasi C. Good features to track. Proceedings of IEEE Conference on Computer Vision and Pattern Recognition (CVPR). 1994:593-600 pp.
**DOI:** 10.1109/CVPR.1994.323794

11. Matveev VV, Raspopov VYa. Fundamentals of Strapdown Inertial Navigation Systems. Saint Petersburg: Elektropribor, 2009;280 p. (In Russ.).

12. Megyesi D, Bréda R, Schrötter M. Adaptive Control and Estimation of the Condition of a Small Unmanned Aircraft Using a Kalman Filter. Energies. 2021;14:2292 p.
**DOI:** 10.3390/en14082292